Fall 2011

Interrelations among leaf and canopy nitrogen, optical and structural traits

Franklin Brown Sullivan
University of New Hampshire, Durham

INTERRELATIONS AMONG LEAF AND CANOPY NITROGEN, OPTICAL AND STRUCTURAL TRAITS

BY

FRANKLIN BROWN SULLIVAN
B.S. Forestry and Earth Systems, University of Massachusetts, 2009

Submitted to the University of New Hampshire
in Partial Fulfillment of
the Requirements for the Degree of

Master of Science
in
Natural Resources: Forestry

September, 2011

This thesis has been examined and approved.

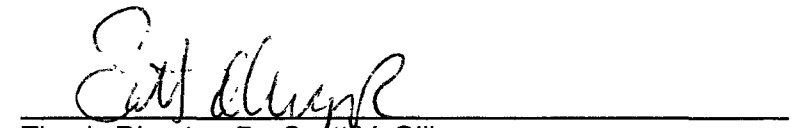

Thesis Director, Dr. Scott V. Ollinger
Professor of Natural Resources
Complex Systems Research Center

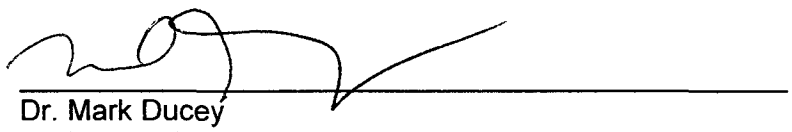

Dr. Mark Ducey
Professor of Natural Resources
Department of Natural Resources and the Environment

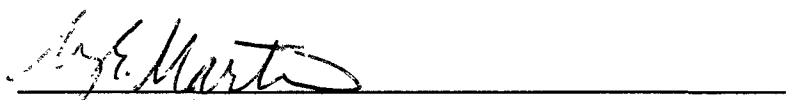

Dr. Mary E. Martin
Research Assistant Professor of Earth, Oceans, and Space
Complex Systems Research Center

August 15, 2011
Date

ACKNOWLEDGEMENTS

First and foremost, I would like to thank my committee: Drs. Scott Ollinger, Mark Ducey, and Mary Martin, for their guidance, support, and encouragement. Scott's dedication to his research program and teaching, all in addition to a busy professional life, is a true inspiration. Mary was always available and didn't mind the occasional (or not so occasional) drop-by, and her help with developing skills in programming were invaluable for not only this project, but my future in ecological research. Mark's assistance in interpreting statistical analyses has been and will be extremely helpful.

Being a part of the Forest Ecosystems Research Group in Complex Systems Research Center has been a pleasure these past two years. Working closely with other members of the lab has not only been easy, but it has been quite fun. I am extremely grateful for their support and assistance in both the field and in the lab. I would like to thank Michelle Day for her assistance in planning and implementing field sampling. Also, I want to thank Lucie Lepine, Haley Wicklein and Andrew Ouimette for their assistance in the field and always being available to talk and share thoughts and new ideas. For their assistance in the lab, I would like to thank Andy's lab crew for summer 2010, and especially Calvin Diessner and Paul Pellissier for their help in both sampling and processing.

Of course I would also like to thank my family and friends for their encouragement and support throughout this whole process. I especially want to acknowledge my parents, for developing an interest in forest ecology (even if it is only because of the wood stove), and Katy Homer, for not going crazy when she would arrive home from work at 11PM and I would neglect to look up from my computer.

I also want to thank David Bartlett for financial support through the New Hampshire NASA Space Grant Consortium. This work was funded by the NH NASA Space Grant Fellowship and a graduate teaching assistantship and Summer TA Fellowship from the University of New Hampshire.

TABLE OF CONTENTS

LIST OF FIGURES

LIST OF TABLES

ABSTRACT

INTERRELATIONS AMONG LEAF AND CANOPY NITROGEN,

OPTICAL AND STRUCTURAL TRAITS

by

Franklin Brown Sullivan

University of New Hampshire, September, 2011

A correlation between canopy nitrogen and albedo has been observed across a wide range of forest types. Determining the nature and mechanisms behind the relationship would help to understand the role of nitrogen in the climate system and better understand forest-climate interactions. The purpose of this study was to examine sources of variation in leaf and canopy optical traits with respect to variation in nitrogen concentrations at both scales.

We found that %N was significantly correlated with leaf and canopy albedo and that both %N and albedo were strongly correlated with forest composition. Many canopy structural traits were found to correlate with each other, as well as with canopy %N and albedo. We hypothesize that a combination of canopy structural attributes are responsible for the correlation between canopy %N and albedo, partially due to their effect on the photon recollision probability.

CHAPTER I

INTRODUCTION

Nitrogen (N) is a key regulator of leaf photosynthetic capacity (Field and Mooney, 1986; Reich *et al.*, 1995) and a growing body of literature has demonstrated that foliar N has a direct bearing on carbon uptake both within and across biomes at leaf and canopy scales (e.g. Reich *et al.*, 1997; Ollinger *et al.*, 2005; Ollinger *et al.*, 2008; Thomas *et al.* 2010). Recently, a correlation between canopy N concentrations (canopy %N) and canopy reflectance has been observed over a variety of temperate and boreal forest types (Ollinger *et al.*, 2008; Hollinger *et al.* 2010). This raises the question of whether N may play an additional, previously overlooked role in the climate system. To date there is little field evidence to support hypotheses regarding the underlying mechanism(s) behind the correlation.

Because forests cover ~30% of the land surface, they have an integral role in the climate system through effects of albedo and surface energy exchange, in addition to their role in the carbon cycle. Recent studies have suggested that the low albedo of forest canopies in boreal regions may have a local warming effect that offsets the climate benefits of carbon uptake in previously deforested regions (Bala *et al.*, 2007). Understanding the drivers of forest canopy albedo may help us to make more knowledgeable management decisions, particularly in light of efforts to mitigate climate change through reforestation and carbon credit systems that do not account for canopy albedo (Thompson *et al.*, 2009). In addition, this may clarify whether N has a direct

influence on climate through its effect on surface energy budgets. If this is the case, an implication is that factors affecting N cycling, such as N deposition may have a direct influence on climate, as well. However, it is unclear the extent to which N is a direct or indirect driver of the relationship observed. This study was designed to address this question by examining relationships between canopy %N and a variety of leaf and canopy level traits that are known to influence albedo.

At the leaf level, photosynthetic pigments, water content, and intercellular air spaces have all been shown to affect reflectance (Gates *et al.*, 1965; Slaton *et al.*, 2001). A positive correlation has been demonstrated between mesophyll cell surface area exposed to intercellular air space per unit leaf surface area (A_{MES}/A) and near-infrared reflectance (Slaton *et al.*, 2001). Some studies have shown that A_{MES}/A is positively correlated with leaf thickness, suggesting a positive relationship between leaf thickness and reflectance (James *et al.*, 1999). Furthermore, thickness and LMA have been shown to be significantly correlated with each other (Niinemets, 1999), but high LMA may also be the result of denser tissues and cellular arrangements in leaves (Wright *et al.*, 2004). Changes in leaf refractive indices, and therefore reflectance, may be related to thickness and density of cells and tissue (Jacquemoud and Baret, 1990), and so may have confounded recent efforts to relate LMA and leaf albedo (Wicklein *et al.*, in review).

It has been hypothesized that changes in leaf traits supporting increased photosynthetic rates would influence canopy albedo through increased backscattering in high N canopies (Hollinger *et al.*, 2010; see Bartlett *et al.*, 2011 and Wicklein *et al.*, in review). However, recent evidence suggests that the relationship between leaf albedo and foliar %N does not cause trends observed at the canopy level, as would be expected if leaf albedo was the sole driver of the canopy %N – albedo relationship (Bartlett *et al.*, 2011; Wicklein *et al.*, in review). Nevertheless, these studies were limited

to broadleaf deciduous species, whereas canopy level studies have been conducted across a broader range of species.

In addition to leaf optical traits, it is possible that the canopy %N – albedo relationship is caused by structural characteristics of stems and forest canopies, which could be directly influenced by physiological responses to N or driven by characteristics that covary with N. Canopy complexity has been measured and modeled in a variety of ways. Although many studies have modeled structural influences on canopy reflectance, few field studies have directly measured and related canopy complexity to canopy albedo (Thompson *et al.*, 2004), and most have modeled structural influences on canopy reflectance. Several studies have incorporated leaf area index (LAI) or related measures as a driving factor in canopy reflectance models (Verhoef, 1984; Jacquemond, 1993; Chen and Leblanc, 1997; Asner, 1998; Smolander and Stenberg, 2003), but field studies have shown mixed results on the role of LAI as a control on canopy reflectance (e.g. Smolander and Stenberg, 2005; Ollinger *et al.*, 2008; Lepine *et al.*, in prep).

Foliage clumping, a measure of the degree to which foliage is grouped within shoots, branches, or a tree crown (Chen and Cihlar, 1995; Niinemets *et al.*, 2002; Smolander and Stenberg, 2003), has been shown in modeling studies to influence canopy reflectance by allowing deeper penetration of radiation into the canopy, with background reflectance contributing increasingly to the overall albedo (Oker-blom and Kellomaki, 1983; Whitehead *et al.*, 1990; Gerard and North, 1997; Chen *et al.*, 2005). Although some studies have reported self-shading and mutual shading of foliage in forests of all types (Gerard and North, 1997), there has been an emphasis on the effects of shoot and branch clumping in evergreens (Oker-Blom and Kellomaki, 1983; Smolander and Stenberg, 2003; Rautiainen and Stenberg, 2005). Broadleaf canopy reflectance has by-and-large been considered to be less strongly influenced by clumping and self-shading at small scales (Smolander and Stenberg, 2003; Rautiainen and

Stenberg, 2005), though self-shading within broadleaf canopies at the branch scale should undoubtedly occur and vary to some extent.

For this study, we used field measurements and high spatial- and high spectral-resolution data from NASA's Airborne Visible/Infrared Imaging Spectrometer (AVIRIS) at two forested sites in New Hampshire: the Bartlett Experimental Forest and the Burley-Demeritt Farm. We characterized canopy structure with common and novel parameters, including leaf area index (LAI), the foliage element clumping index (CI), gap fraction (GF), the number of leaves per cubic meter, canopy equivalent water thickness (EWT_C) and leaf mass per unit ground area (LMA_C).

CHAPTER II

MATERIAL AND METHODS

Study Sites

The study was conducted at two sites in New Hampshire, Bartlett Experimental Forest (BEF) and Burley-Demeritt Farm (BDF; Figure 1). Leaf samples, species composition, and hemispherical photographs were collected from 13 plots at BEF and four plots at BDF. Plots were chosen after preliminary field investigations ranging in site characteristics including species composition, canopy %N estimates, and canopy albedo. The four plots at BDF were selected in order to include white pine and red oak, species that were of interest to our study, but do not occur in appreciable densities at BEF, and to examine if canopy structure – albedo relationships would hold across sites within New Hampshire. Spectral, chemical, and structural characteristics were measured and estimated at leaf and canopy scales on each plot using field and lab methods and AVIRIS imagery.

BEF is located in White Mountain National Forest in Bartlett, NH. The forest is a 1052 ha research and demonstration forest established in 1932 by the United States Forest Service. Soils are coarse textured and of granitic drift in origin, ranging from shallow weathered bedrock to outwash and compact sediments, to basal tills and washed ablational tills. Elevations within the experimental forest range from 200 to 850 m, with precipitation averaging between 120 and 140 cm annually and a mean annual temperature of ~8°C (Smith and Martin, 2001). The forest is composed of northern hardwoods, secondary successional deciduous and coniferous forest species including

red spruce (*Picea rubens* Sarg.) and balsam fir (*Abies balsamea* (L.) Mill.), American beech (*Fagus grandifolia* Ehrh.), red maple (*Acer rubrum* L.), sugar maple (*Acer saccharum* Marsh.), Eastern hemlock (*Tsuga canadensis* (L.) Carrière), yellow birch (*Betula alleghaniensis* Britton), white pine (*Pinus strobus* L.) and red oak (*Quercus rubra* L.). In 1932, prior to establishment as a research forest, a grid of 500 1/10 ha (32x32m) plots were established through the forest (Leak and Smith, 1996).

The University of New Hampshire currently operates BDF as a research organic dairy farm located in Lee, NH. The property, including approximately 200 acres of woodlands, was purchased in 1969. Precipitation averages around 110 cm annually with a mean annual temperature of ~9°C (Ollinger *et al.*, 1995). Twenty-three seven meter radius plots were established in the wooded area of BDF in 2008 for a sustainable biomass harvesting study (Aber *et al.*, unpublished).

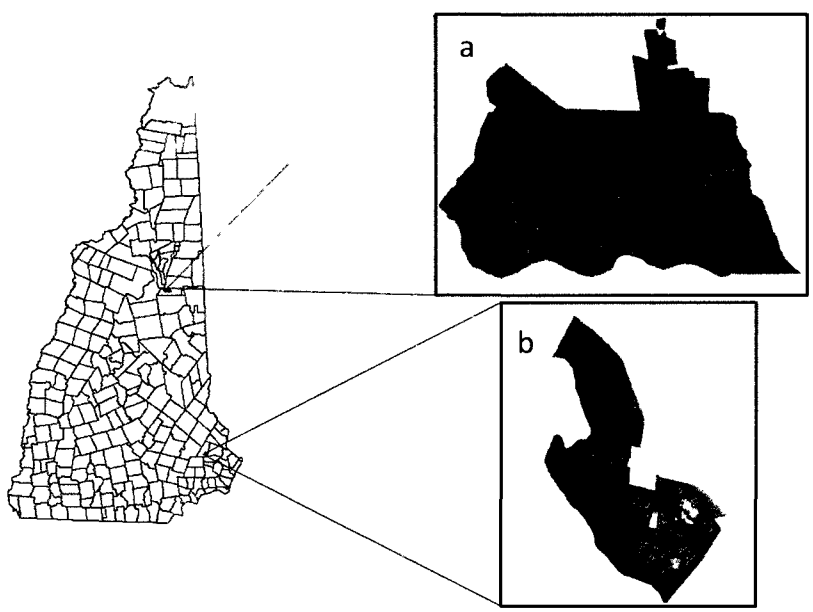

Figure 1 Bartlett Experimental Forest, White Mountain National Forest, Bartlett, NH (a) and Burley-Demeritt Farm, Lee, NH (b). Thirteen plots at BEF and four plots at BDF were sampled (marked in red). Not to scale.

Field Sampling

Species composition by percent of total leaf area (from here on species composition) was determined using a camera mounted on a tripod with a telephoto lens calibrated to distance used as a rangefinder (Aber, 1979; Smith and Martin, 2001). A 15-point gridded focusing screen was used for sampling points. For each grid intersection, the species and the height to the lowest focused leaf were recorded; if no species appeared on a grid-point throughout the depth of the canopy, an observation of open sky was recorded. On each plot, there were nine sampling locations, one at the center of the plot and the rest 10m from center in each of the cardinal and off cardinal directions, for a total of 135 sampling observations (9 locations x 15 obs./loc.). In addition to species composition, measurements were used for calculating canopy chemistry as described by Smith and Martin (2001), as well as the vertical distribution of foliage throughout the canopy (Aber, 1979).

Foliage samples were collected during the growing season from between four to eight dominant and codominant trees on each plot at both BEF and BDF between mid-July and early August, 2010. Several leaves were collected from three height classes from trees in each plot: lower, middle, and upper canopy. The height from which each sample was collected was recorded using a digital hypsometer (Haglöf Vertex) to complete analysis of leaf structure variability with height. Foliage was collected using a 12 gauge shotgun with 1.25 ounce 2.75 inch cartridges loaded with #3 steel shot. Samples were stored with moist paper towels in ziplock plastic bags in a cool storage container and returned to the Forest Ecosystems Lab at Morse Hall in Durham, NH for spectral, chemical, and structural measurements.

To estimate LAI, CI, and GF, digital hemispherical photos were collected from each plot using a Nikon CoolPix 4500 equipped with a fisheye lens on a self-leveling monopod at approximately breast height (1.3m above ground). Five photos were

collected from each plot, one from the plot center and from each of the four cardinal directions. Photos were taken at dusk or just before dawn with a sun angle approximately <15° above the horizon for diffuse and uniform backlighting of trees and foliage to retrieve accurate measurements. Measurements were taken according to the FluxNet Canada protocol as outlined by Zhang *et al.* (2005). The camera was set to "manual" and set to fine resolution mode (2272x1704). Before entering the forest or under a large gap in the canopy, the exposure was determined by holding down the shutter button and setting the exposure two steps faster than the automatically set exposure setting (i.e., with a gap exposure setting of 1/500, the exposure was manually set to 1/125 for photographs under the canopy). This was done to ensure contrast between foliage and sky. Photographs were backed up to a computer each night after sampling and labeled according to plot and sampling location.

Spectral Analysis

Remote Sensing Data

The AVIRIS instrument collected image data along northeastern transects in July, 2009. Flown on the ER-2 aircraft, the sensor collects data in 224 contiguous wavelengths from 350 to 2400nm, with a nominal spectral resolution of 10nm, a swath width of approximately 11km and a pixel size of ~17m. Scenes were orthorectified by NASA's Jet Propulsion Lab, and delivered as calibrated radiance data ($\mu W/cm^2/nm/sr$). Radiance images were transformed to apparent surface reflectance using the ACORN (v.5) atmospheric correction program (ImSpec, LLC).

Lab Data

Upon return to the lab, samples were stored in one gallon zipped plastic storage bags and refrigerated to be kept fresh. Within the week, leaf spectra of fresh samples from the upper canopy were obtained using a bench-top visible and near-infrared spectrophotometer (NIRS; Foss NIRSystems 6500, Eden Prairie, MN). The NIRS has a

spectral range of 400nm to 2500nm, with a spectral resolution of 10 nm and sampling interval of 2nm. Optically dense layers of leaves were scanned using the NIRS to approximate a forest canopy lacking structure, and to reduce the likelihood of transmission of light through all leaf layers. To do this, six approximately 11.5 cm^2 discs were cut from deciduous leaves and a subsample of needles from each sampled tree were removed from stems and packed into the quartz sampling cup of the NIRS. For each sample, discs and needles were scanned, shuffled, and rescanned for a total of three sample spectra. Reflectance spectra from each scan were averaged for a single spectral signature curve per sample.

A generic solar spectrum file was generated from the SMARTS v.2.9.5 software (Solar Consulting Services, 2005, 2006) with minimum and maximum wavelengths of 400nm and 2500nm, respectively, and 2nm spectral resolution. Because spectral resolution of the solar spectrum file degraded at 1700nm, spline interpolation was performed to improve spectral resolution from 10nm to 2nm in part of the mid-infrared region (1700-2500nm). Leaf albedo was calculated by integrating the reflected energy flux for each sample from 400nm to 2500nm and dividing by the integral of the energy flux of the solar spectrum. Canopy albedo was calculated using image spectra from AVIRIS with the same method used to calculate leaf albedo. In addition, visible (400-700 nm), near-infrared (NIR; 700-1300 nm), and mid-infrared (MIR; 1300-2500 nm) leaf albedo were calculated for each upper canopy sample by integrating the energy flux for the sample for the wavelengths of interest and dividing by the integral of the energy flux of the solar spectrum over the same region.

Mean canopy reflectance and a ratio of leaf to canopy reflectance ($F_{L\text{-}C}$) were calculated for the visible and NIR. $F_{L\text{-}C}$ was calculated by dividing leaf reflectance by canopy reflectance for each wavelength, then averaging factors across visible and NIR. Portions of the spectrum were excluded from these calculations because of water

absorption features (1200-1300 nm), and noise in the red edge (700-800 nm) and the low visible wavelengths in AVIRIS imagery (400-450 nm). FL-C in the NIR region quantifies the influence of canopy elements larger than leaves on albedo. The results of this analysis will help us to attempt to determine relevant canopy structural traits to canopy albedo.

Chemical and Structural Analysis

Leaf Level

For each sample of broadleaf deciduous leaves, the total number of leaves (L_N) was counted in order to estimate mean leaf surface area. The total sample was weighed and approximately twenty 2.035cm^2 leaf punches were taken from each foliage sample and weighed. Samples were dried for at least 48 hours in a 70°C oven, and then reweighed. Leaf punches were reweighed after 48 hours of drying for calculation of leaf mass per unit area (LMA) and for determining moisture content and equivalent water thickness (EWT; cm). Mean leaf surface area (L_A) was calculated using Eq. 1:

$$L_A = \left(\frac{1}{LMA} * S_{dw}\right)/L_N \qquad \textbf{[Eq. 1]}$$

where S_{dw} is the dry weight of the entire sample, including leaf punches and the remaining foliage.

For needle leaf species, subsamples of between 10 and 25 needles were removed from the stems of each foliage sample and weighed. Needles were laid on a table with an opaque surface, backlit by three 14 watt Ecosmart bulbs in 8 inch reflective shells to create maximum contrast between needles and background. Needles were photographed using a Nikon D90 DSLR camera fixed and leveled to a rigged copy stand set approximately one foot above the surface of the table. Calibration was performed periodically with objects of known size (two quarters) in order to avoid errors from slight changes in camera position. Needle images were analyzed to determine total needle

area for each subsample by dividing the total number of pixels above a given threshold in each of the images to the total number of pixels above the threshold in the calibration images and multiplying by the known calibration size. L_A was estimated by dividing the total area of the subsample needles by the number of subsample needles. Needles removed from stems were dried at 70°C for at least 48 hours and reweighed to determine moisture content and LMA. Remaining foliage was oven dried for chemical analysis.

Dried samples were ground using a Wiley mill and passed through a 1mm mesh screen. Ground samples were dried again prior to being analyzed for mass-based foliar nitrogen concentrations (foliar %N; grams nitrogen per 100 grams of foliage) using the NIRS. Average spectral signatures from two scans of ground material from each sample were used to predict foliar nitrogen and lignin concentrations following the method described by Bolster *et al.* (1996).

Canopy Level

Hemispherical photos were analyzed using DHP version 4.5 and TRACWin version 4.0.1 (Natural Resources Canada), using methods described by Leblanc (2006). Images were imported in JPEG format from the camera. Five images were analyzed for each plot. Thresholds were set manually in DHP for each photo and processed to extract a TRAC-like profile for analysis in TRACWin to determine LAI and gap fraction estimates for each plot. For analysis, Gamma was set to 2.2 for all photos. The TRAC-like profiles produced in DHP were analyzed using TRACWin in the automated DHP mode. Estimates of needle-to-shoot area ratios and woody-to-total plant area ratios were used based on the species composition of each plot and values for different species and stand types from the literature (Gower *et al.*, 1999). For types that were not available in the literature, estimates were based on stand age, structure, and

composition. LAI and clumping index values were calculated based on Miller's theorem, integrating values from view angles of 10° to 80°.

Foliage height profiles were generated for whole stands and for individual species on each plot using a modified version of the method described by Aber (1979, see Smith and Martin, 2001). Profiles were generated based on Eq. 2, derived from Aber (1979):

$$y = \ln(N_{f1} - N_{f2}) \qquad \textbf{[Eq. 2]}$$

where f1 and f2 are the lower and upper heights of the region of the canopy that is in question, and N_{f1} and N_{f2} are the number of observations above f1 and f2 (Aber, 1979). The proportion of LAI for a given region is calculated as y for that region divided by the y of the whole canopy. Species profiles were generated by calculating the proportion of observations for each species within a canopy region of interest relative to the total number of observations in the canopy region. Profiles were generated for 2m canopy regions to capture as much variability as possible in species distributions throughout the canopy while still providing a realistic distribution of foliage area. Because estimates of absolute LAI (i.e., whole canopy y) using this method have been found to be inaccurate (Aber, 1979), estimates derived from hemispherical photography were applied to determine actual LAI for each canopy region. The proportion of total LAI was calculated for each species, and % deciduous was calculated by summing LAI proportion for only deciduous species.

We estimated the number of leaves per cubic meter using methods similar to Parker *et al.* (1989). Regression relationships between L_A and canopy height were determined for each species on each plot. When significant, L_A for each canopy region was estimated, otherwise whole canopy averages of L_A were used for each species.

The number of leaves in each canopy region was calculated from LAI and L_A of each region using equation 3:

$$\#\frac{leaves}{m^2} = \left(\frac{LAI}{LA}\right) \qquad \textbf{[Eq. 3]}$$

and the number of leaves per cubic meter was estimated by summing all canopy regions and dividing by the height of the canopy.

Mass-based canopy nitrogen concentrations (canopy %N) were calculated as a weighted average of foliar %N of each species (weighted by foliar biomass proportion, see Smith and Martin, 2001). Average L_A and leaf albedo (from here on mean leaf albedo) were estimated by calculating weighted averages (by LAI proportion). LMA_C and EWT_C were estimated by calculating weighted averages (by LAI proportion) and multiplying by LAI. For calculating weighted averages, when species were not sampled on a plot, values were estimated by averaging all samples of that species. Leaf albedo for species that were not sampled were estimated from a multiple linear regression model using literature estimates of foliar %N and LMA (Foliar Chemistry Database, http://www.folchem.sr.unh.edu/), as well as species type (evergreen=1 and deciduous=0), an interaction of foliar %N and LMA, and an interaction of foliar %N and species type. In the same vein, mean leaf reflectance for each wavelength was also calculated on each plot for comparing leaf-level and plot-level reflectance.

Statistical Analysis

Statistical analysis was performed and graphs and figures were generated in R version 2.11.1 (R Foundation for Statistical Computing, 2010). Regression analysis was performed to determine relationships between height and average leaf area of samples for each species on each plot. Stepwise multiple regression analysis using stepAIC in R was performed to predict leaf albedo from leaf chemical and structural characteristics of foliage samples. Random effects of plots and species were accounted for using lmer in

R. To prevent overfitting of plot level albedo models, a selection of variables were included in stepwise multiple regression analysis a priori based on Spearman's rho from correlation analysis of canopy albedo and individual plot variables. Shapiro-Wilk normality and non-constant variance score tests were performed to determine if data were normally distributed prior to analysis. When necessary, log transformations were performed to correct for skew. Tukey's post-hoc Honest Significant Difference test was used on functional type to determine if leaf level trends could be driven by significant differences between functional types.

CHAPTER III

RESULTS

Leaf Level

Leaf Structure and Nitrogen

Leaf EWT was found to be significantly and negatively correlated with foliar %N (r^2=0.66, p<.001, RMSE=0.006; Figure 2a), and negatively correlated with N_{area} (r^2=0.68, p<.001, RMSE=0.006; foliar N_{area} equals %N x LMA). LMA was found to correlate strongly and negatively with foliar %N (r^2=0.71, p<.001, RMSE=48.9; Figure 3a), and positively with N_{area} (r^2=0.65, p<.001, RMSE=53.56). Marginally significant positive trends between L_A and foliar %N were observed within deciduous species (r^2=.04, p<.05, RMSE=23.39), and within evergreen species (r^2=.12, p<.01, RMSE=0.068). Foliar N, EWT, and LMA were significantly different between functional types (for all, p<.001). See Table 1 for a summary of leaf structure, %N, and albedo correlation analysis.

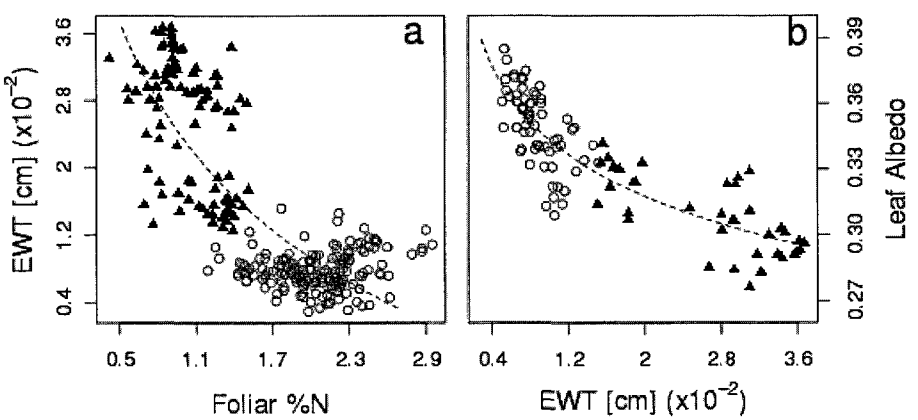

Figure 2 Relationships between EWT and foliar %N (a) and leaf albedo (b) for needle-leaved evergreen conifers (black triangles) and broadleaf deciduous species (open circles). Regression relationships for pooled species are: EWT=234.3-204.4*(log(%N)) and albedo=0.515-0.037*(log(EWT)).

Table 1 Intercorrelation among leaf nitrogen and optical and structural traits. Reported values are Spearman's ρ. All are significant at p<.001

	LMA	EWT	L_A	Leaf %N	N_{area}
EWT	0.936				
L_A	-0.751	-0.763			
Leaf %N	-0.738	-0.684	0.743		
N_{area}	0.845	0.814	-0.505	-0.332	
Full albedo	-0.885	-0.867	0.502	0.511	-0.795
Visible albedo	0.431	0.421	-0.648	-0.773	-0.039
NIR albedo	-0.895	-0.870	0.549	0.571	-0.752
MIR albedo	-0.948	-0.951	0.647	0.678	-0.724

Full Spectrum Leaf Albedo

Within functional types (broadleaved deciduous and needle-leaved evergreen), two distinct relationships were found between foliar %N and albedo. Evergreen needles exhibited a significant positive relationship between foliar %N and albedo (r^2=0.23, p<.001, RMSE=.015) and deciduous leaves showed a significant negative relationship (r^2=0.21, p<.001, RMSE=.015). Pooling deciduous and evergreen functional types resulted in a significant positive trend between foliar %N and albedo (r^2=0.31, p<.001, RMSE=.022, Figure 3b). Foliar N_{area}, however, was negatively correlated with leaf albedo (r^2=0.59, p<.001, RMSE=.016). Negative relationships between leaf albedo and LMA were found for both evergreen (r^2=0.59, p<.001, RMSE=.011) and deciduous leaves (r^2=0.49, p<.001, RMSE=.012), as well as for both types pooled (r^2=0.79, p<.001, RMSE=.012; Figure 3c). Leaf albedo was found to be significantly and negatively correlated with leaf EWT (r^2=0.76, p<.001, RMSE=.013; Figure 2b).

A multiple regression including foliar %N, functional type, LMA, and interactions between foliar %N and functional type and LMA and functional type was significant (pseudo r^2=0.86, see Table 2 for AIC results). After accounting for random effects of plots and species, fixed effects account for 86% of explained variation, while plots and species account for 1.1% and 3.1% of the variation, respectively. Remaining variation in

these data is from the true residual, accounting for the remaining 9.8% of the variability. Because the goal of this study was to investigate canopy %N and albedo, from here on, only foliar %N relationships will be presented and discussed.

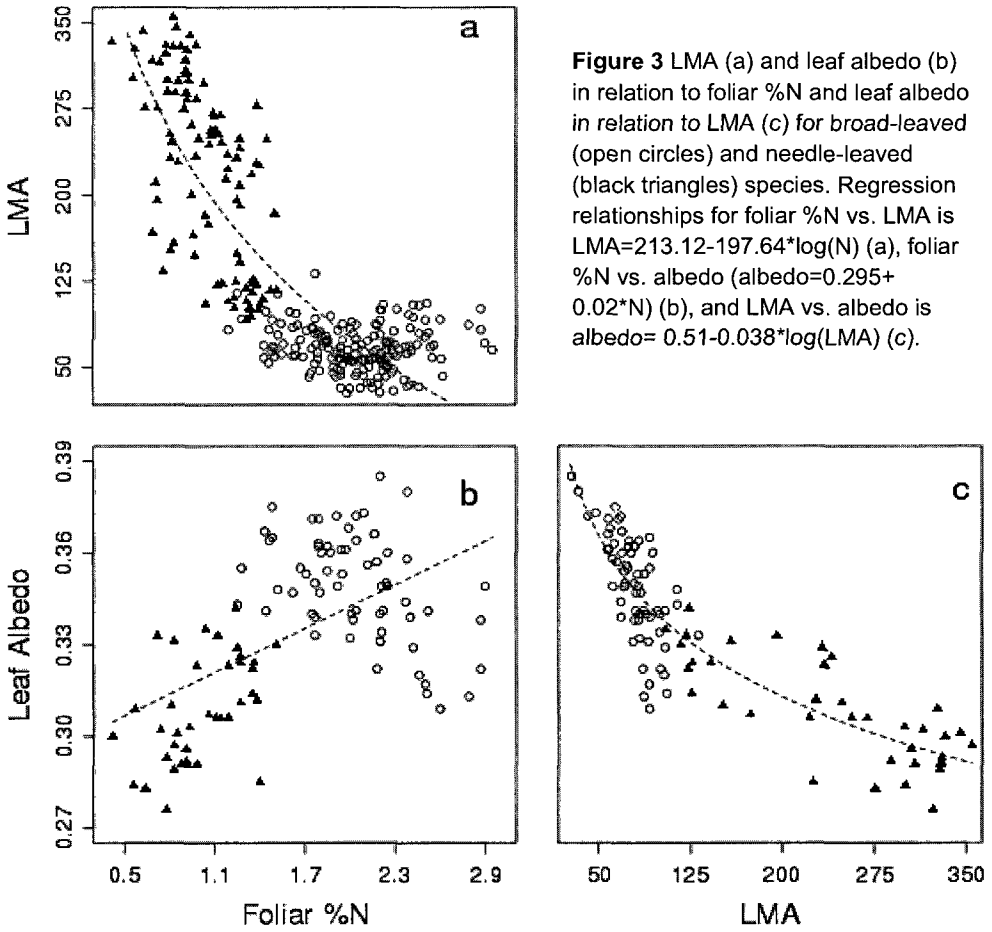

Figure 3 LMA (a) and leaf albedo (b) in relation to foliar %N and leaf albedo in relation to LMA (c) for broad-leaved (open circles) and needle-leaved (black triangles) species. Regression relationships for foliar %N vs. LMA is LMA=213.12-197.64*log(N) (a), foliar %N vs. albedo (albedo=0.295+ 0.02*N) (b), and LMA vs. albedo is albedo= 0.51-0.038*log(LMA) (c).

Leaf Albedo for individual spectral regions

In the visible region, there was a significant negative relationship between foliar %N and albedo (r^2=0.54, p<.001, RMSE=.007). The addition of LMA improved the relationship (r^2=0.61, p<.001, RMSE=.006); however, functional type and a functional type – foliar %N interaction were not significant.

In the NIR region, significant trends were present with all variables. Foliar %N was positively correlated with NIR albedo, and alone explained 39% of the variation (RMSE=.040) and LMA explained 76% of the variation and was negatively correlated

with NIR albedo (RMSE=.025). In a multiple regression, all three variables were significant, along with two interaction terms between functional type and foliar %N and type and LMA (pseudo r^2=0.86). After accounting for random effects of plots and species, fixed effects account for 86% of explained variation, while plots and species account for 1.5% and 0.4% of the variation, respectively. Remaining variation in these data is from the true residual, accounting for the remaining 12.1% of the variability.

A significant trend resulted from a simple linear regression between MIR albedo and LMA (negative, r^2=0.80, p<.001, RMSE=.024) and with foliar %N (positive, r^2=0.50, p<.001, RMSE=.039). A stepwise multiple regression of MIR albedo on LMA, species type, foliar %N and interactions resulted in the removal of all variables except for species type, LMA, and a species type – LMA interaction (pseudo r^2=0.87). After accounting for random effects of plots and species, fixed effects account for 87.3% of explained variation, while plots and species account for 0% and 7.3% of the variation, respectively. Remaining variation in these data is from the true residual, accounting for the remaining 5.4% of the variability. See Table 2 for a summary of full- and sub-spectrum albedo results.

Table 2 Multiple regression results for leaf level analysis of full spectrum albedo, visible, NIR, and MIR albedo with foliar characteristics of all species pooled. Values reported are ΔAIC

Spectral Region	Foliar %N, LMA, Type	LMA, Type, LMA:Type	Foliar %N, LMA, Type, %N:Type, LMA:Type	Foliar %N, LMA, Type, LMA:Type, %N:LMA	r^2
Full	41.46	39.71	**0**	2.58	0.86
Visible	5.86	57.5	1.38	**0**	0.64
NIR	24.24	20.69	**0**	2.09	0.85
MIR	68.44	4.63	**0**	2.25	0.91

ΔAIC is the difference between the best model (ΔAIC=0) and alternative models, larger AIC indicates poorer fit model.

Canopy Level

Canopy Nitrogen, Reflectance and Albedo

Canopy level attributes are reported in Table 3. Field measured canopy %N was significantly positively correlated with canopy albedo (r^2=0.67, p<.001, RMSE=.023; Figure 4a) across all plots and sites in this study. Analysis of canopy %N at BEF resulted in a slightly better fit (r^2=0.76, p<.001, RMSE=.022); although, the slope remained similar.

Table 3 Summary of relevant canopy structural characteristics for each plot sampled. Plots with letters BD were sampled at BDF, remaining plots were sampled at BEF.

Plot	Canopy albedo	%N	% Deciduous	Mean leaf albedo	LAI	CI	GF	Leaves/m^3	EWT_C	LMA_C
10T	0.14	0.89	0.20	0.32	2.92	0.95	0.38	9224	.068	681.1
14BD	0.18	1.55	0.56	0.32	3.01	0.95	0.24	2341	.053	421.5
14Z	0.24	1.89	0.97	0.34	2.71	0.98	0.14	275	.019	180.6
21BD	0.15	1.25	0.31	0.34	6.47	0.95	0.09	7292	.136	1043.1
24M	0.22	1.88	0.97	0.36	3.20	0.94	0.06	356	.028	205.9
26BD	0.17	1.26	0.15	0.32	4.53	0.95	0.20	6725	.111	905.7
32P	0.16	1.36	0.47	0.34	3.58	0.97	0.15	8275	.045	363.4
34K	0.15	1.51	0.47	0.34	3.19	0.96	0.13	6184	.037	312.5
5D	0.22	2.27	1.00	0.34	2.31	0.99	0.15	32	.017	157.0
6N	0.13	1.00	0.18	0.31	2.31	0.87	0.29	6721	.063	581.0
7N	0.15	0.98	0.43	0.32	2.16	0.92	0.27	4623	.045	422.4
9BD	0.18	2.16	0.97	0.34	2.29	0.97	0.09	125	.019	157.7
9D	0.23	1.89	1.00	0.35	3.03	0.98	0.09	61	.021	189.4
A2B	0.21	1.54	0.93	0.35	3.37	0.98	0.13	797	.028	244.0
B1B	0.20	1.24	0.71	0.35	2.67	0.96	0.11	4481	.032	277.1
ES1	0.23	2.33	1.00	0.34	2.29	0.98	0.31	129	.025	173.8
ES2	0.24	2.34	1.00	0.34	2.49	0.96	0.20	95	.025	173.4

LAI = leaf area index (m^2/m^2)
CI = clumping index
GF = gap fraction (%)
EWT_C = equivalent water thickness (cm)
LMA_C = leaf mass per unit ground area (g/m^2)

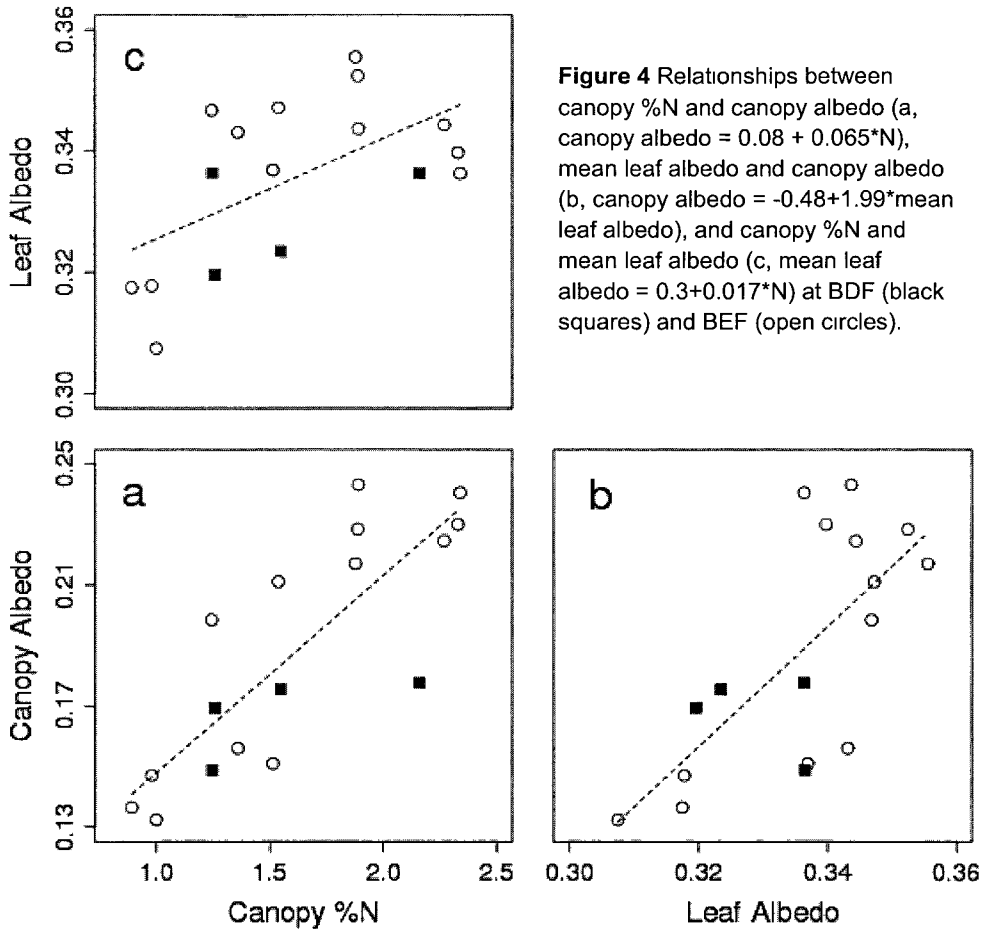

Figure 4 Relationships between canopy %N and canopy albedo (a, canopy albedo = 0.08 + 0.065*N), mean leaf albedo and canopy albedo (b, canopy albedo = -0.48+1.99*mean leaf albedo), and canopy %N and mean leaf albedo (c, mean leaf albedo = 0.3+0.017*N) at BDF (black squares) and BEF (open circles).

Mean NIR reflectance was found to be significantly and positively correlated with canopy %N (r^2=0.70, p<.001, RMSE=.053). A weaker but still positive relationship was found between MIR reflectance and canopy %N (r^2=0.46, p<.001, RMSE=.004). Mean visible reflectance was not significantly correlated with canopy %N or canopy albedo. Mean leaf albedo was significantly and positively correlated with canopy %N (r^2=0.34, p<.05, RMSE=.011; Figure 4c) and canopy albedo (r^2=0.50, p<.001, RMSE=.028; Figure 4b), although mean leaf albedo was consistently higher than canopy albedo. We calculated NIR $F_{L\text{-}C}$, a ratio of leaf to canopy NIR reflectance, which is an aggregate measure describing the influence of branch- to canopy-level factors. Strong negative relationships between NIR $F_{L\text{-}C}$ and canopy %N and % deciduous were found (Figure 5; r^2=0.63, p<.001, RMSE=0.18 and r^2=0.70, p<.001, RMSE=0.16, respectively).

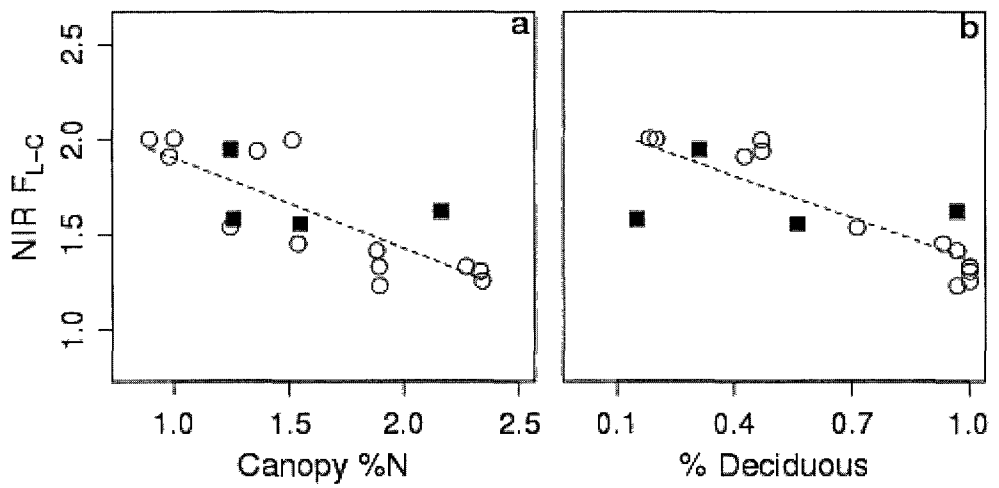

Figure 5 Mean NIR F_{L-C} as a function of %N (a, F_{L-C} = 2.38-0.4759*N) and % deciduous (b, F_{L-C} = 2.1-0.73*%deciduous) for plots at BDF (black squares) and BEF (open circles).

Structure and Composition with Albedo and Nitrogen

We found no significant relationship between LAI and canopy albedo or canopy %N. In addition, $LAIm^{-3}$ also showed no significant relationship with canopy albedo or canopy %N. Furthermore, $LAIm^{-3}$ in the top half of the canopy was not related to canopy albedo nor canopy %N. On the other hand, derived from DHP and LAI, a significant positive relationship was found between clumping index and both canopy albedo (r^2=0.39, p<.01, RMSE=.031) and canopy %N (r^2=0.36, p<0.05, RMSE=.023), indicating that increased grouping (lower clumping index value, i.e. non-random distribution) of canopy elements corresponded with lower canopy albedo. Canopy gap fraction did not significantly relate to canopy albedo or canopy %N.

Canopy variables and % deciduous were found to be significantly correlated (see Table 4). Mean leaf albedo and % deciduous were significantly and positively correlated (r^2=0.57, p<.001, RMSE=.009). Both canopy albedo and canopy %N were also significantly positively correlated with % deciduous (r^2=0.79, p<.001, RMSE=.018 and r^2=0.76, p<.001, RMSE=.246, respectively; Figure 6). Percent deciduous and the number of leaves per cubic meter were strongly negatively correlated (r^2=0.87, p<.001,

1275). Clumping index and % deciduous were significantly related, with increased clumping corresponding to lower % deciduous (r^2=0.39, p<.01, RMSE=.023).

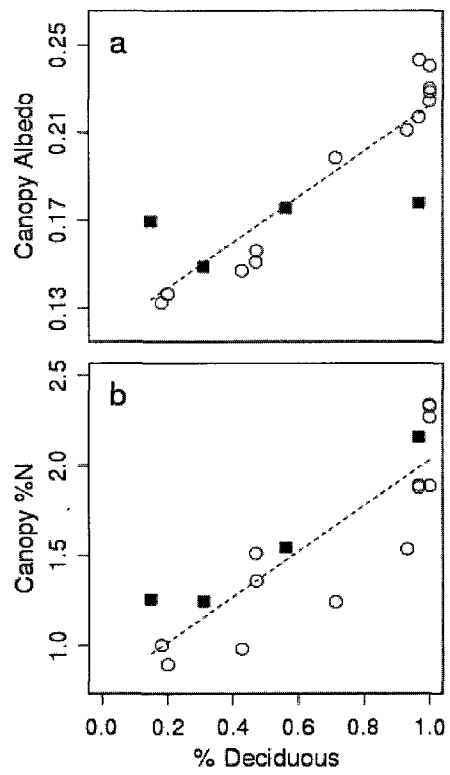

Figure 6 Relationships between % deciduous and canopy albedo (a) and %N (b) at BDF (black squares) and BEF (open circles). Regression relationships are: %N = 0.76+1.27*%deciduous and albedo = 0.118+0.104*%deciduous.

Mean leaf surface area was significantly and positively correlated with both canopy albedo (r^2=0.47, p<.01, RMSE=.029) and canopy %N (r^2=0.54, p<.001, RMSE=9.91). Canopy albedo was negatively correlated with LMA_C (r^2=0.47, p<.01, RMSE=.029), and LMA_C and canopy %N were also negatively correlated (r^2=0.48, p<.01, RMSE=201.6). Canopy albedo was negatively correlated with EWT_C (r^2=0.39, p<.01, RMSE=.031), and EWT_C and canopy %N were also negatively correlated (r^2=0.37, p<.01, RMSE=.027). Canopy albedo and canopy %N were significantly and negatively correlated with the number of leaves per cubic meter (r^2=0.75, p<.001, RMSE=1855 and r^2=0.73, p<.001, RMSE=.020, respectively, see Figure 7). For a summary of correlation analysis, see Table 4.

Multiple Regression Analysis

Results of exploratory multiple regression analysis was consistent with the hypothesis of this study. It was anticipated that canopy albedo would be correlated to one or multiple structural traits that would also correlate canopy %N. Based on analysis of individual variables, the following were selected for inclusion in a stepwise multiple regression analysis: the number of leaves per cubic meter, clumping index, mean LMA,

canopy EWT and mean leaf albedo. Percent deciduous represents an aggregate of structural variables, and so was excluded from analysis. Stepwise regression resulted in a two variable model using the number of leaves per cubic meter and clumping index to predict canopy albedo (r^2=0.79, p<.001, RMSE=.018; see Figure 8).

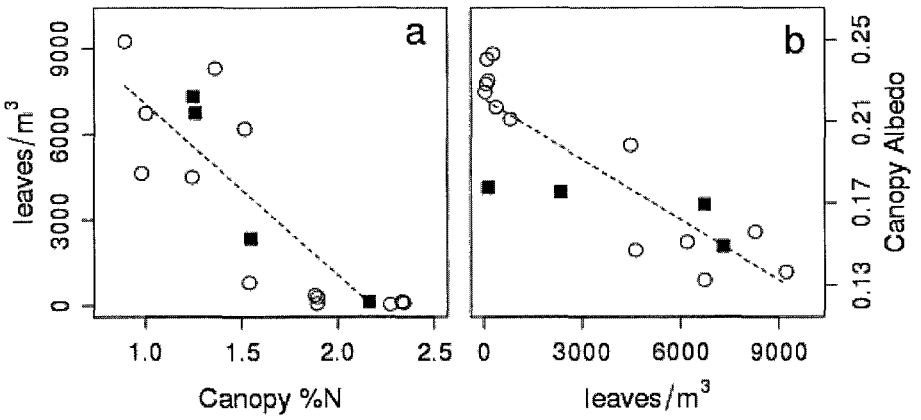

Figure 7 Number of leaves/m^3 vs. canopy %N (a) and albedo (b) for plots at BDF (black squares) and BEF (open circles). Regression relationships are: #leaves/m^3 = 13037.8-5997.3*N, canopy albedo = 0.221-0.0000098*# leaves/m^3

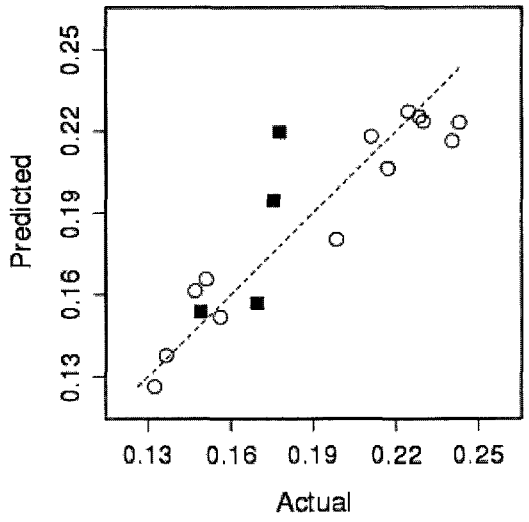

Figure 8 StepAIC results plotted as predicted vs. actual albedo for BDF (black squares) and BEF (open circles), shown here with a 1:1 line (canopy albedo = -.1613 + 0.39*CI - .00000834*#leaves/m^3)

Table 4 Correlation matrix for all canopy variables included in the study. Values shown here are Spearman's ρ.

	% Deciduous	Canopy %N	Albedo	Leaf albedo	LAI	CI	GF	Leaves/m^3	Mean L_A	EWT
Canopy %N	0.878***									
Albedo	0.908***	0.860***								
Leaf albedo	0.661**	0.444	0.662**							
LAI	-0.327	-0.228	-0.140	0.277						
CI	0.719**	0.613**	0.676**	0.622**	-0.071					
GF	-0.259	-0.195	-0.260	-0.679**	-0.431	-0.252				
Leaves/m^3	-0.909***	-0.855***	-0.826***	-0.493*	0.458	-0.590*	0.245			
Mean L_A	0.805***	0.703**	0.743***	0.635**	-0.196	0.657**	-0.434	-0.794***		
EWT	-0.900***	-0.806***	-0.819***	-0.588*	0.429	-0.769***	0.276	0.892***	-0.838***	
LMA	-0.920***	-0.873***	-0.814***	-0.529*	0.475	-0.698**	0.222	0.904***	-0.794***	0.968***

*p<.05, **p<.01, ***p<.001

CHAPTER IV

DISCUSSION

Leaf Level

The goal of this study was to investigate possible mechanisms behind the canopy %N – albedo correlation, including relations between %N and albedo at the leaf level. At the leaf level, the negative relationship between LMA and foliar %N agrees well with those found in previous research (Reich *et al.*, 1995; also see Figure 2). Globally, the causality of N – LMA relationships are complex and unclear (Wright *et al.*, 2004), possibly driven by a latent variable such as A_{MES}/A (Slaton *et al.*, 2001; Shipley *et al.*, 2006), which may result from water limitations (Niinemets, 2001). On a more local scale, these relationships are more likely driven by trade-offs between internal structure and leaf longevity (partially due to climate adaptations) across functional groups (Reich *et al.*, 1995; Niinemets, 2001).

We also found that LMA, EWT, and foliar %N are all correlated with leaf albedo and with each other. Recent studies have found negative correlations between foliar %N and albedo within deciduous species (Wicklein *et al.*, in review; Bartlett *et al.*, 2011). Our results are consistent with this for deciduous species, but across deciduous and evergreen species, a positive correlation similar to those observed at the canopy level was found. The correlation between foliar %N and albedo could be due to an NIR absorption feature of leaf proteins (Johnson, 2001) or to covariation between %N and structural traits of leaves that may directly influence NIR reflectance. Across a wide range of species, we found a strong negative correlation between LMA and leaf albedo.

Changes in LMA may be caused by changes in a latent variable, such as A_{MES}/A, which has been shown to influence internal scattering and absorption in leaves (Slaton *et al.*, 2001). Leaf traits like thickness, density, cell size, organization, and intercellular air space may also directly affect leaf albedo, but the differing influences of each on LMA may have been a confounding factor in earlier studies investigating LMA and albedo (Niinemets, 1999; Slaton *et al.*, 2001; Serrano, 2008; Wicklein *et al.*, in review). Because needles were smaller than the sampling window of the NIRS, it is possible that among evergreen species this relationship was partially caused by external structure (i.e. leaf cross sectional shape, leaf cuticle thickness, bicoloration, and waxes and resins; Slaton *et al.*, 2001; Serrano, 2008); however, the relationship was similar when the effect of external structure was controlled for in deciduous leaves. Internal structure is thought to be important in light and carbon dioxide processing and for maximizing photosynthesis (James *et al.*, 1999), and these changes may also directly effect leaf albedo (Gates et al., 1965; Slaton et al., 2001).

Canopy Level

The data presented in this study suggest a convergence of chemical, structural and optical traits at different scales in forest canopies, which complicates our ability to identify the scattering effects of individual structural traits. Most traits we measured vary consistently across a gradient from low % deciduous to high % deciduous. Earlier studies have shown that both forest composition and canopy chemistry can be predicted based on canopy reflectance (Martin *et al.*, 1997; Roberts *et al.*, 2004; Ollinger and Smith, 2005; Castro-Esau *et al.*, 2006), but these studies did not explore the underlying causes of covariation. The relationship identified between canopy %N and % deciduous is not new; Ollinger and Smith (2005) found similar relationships between forest composition and AVIRIS estimates of canopy %N. In the same vein, mean leaf albedo was found to be significantly and positively correlated with % deciduous, as greater

proportions of foliage with generally higher albedo should result in higher mean leaf albedo. What makes this relationship notable is that mean leaf albedo is consistently higher than canopy albedo in a predictable way.

Like Asner (1998), we found that visible $F_{L\text{-}C}$ (a comparison between leaf and canopy reflectance) was higher than NIR $F_{L\text{-}C}$ (approximately 2.7-4.5 vs. 1.2-2.0), indicating that leaf properties were less directly expressed at the canopy level in the visible region. In the visible region, low canopy reflectance is primarily due to dark materials, such as shaded leaves, wood, non-photosynthetic vegetation, and the ground, which are introduced at scales larger than the leaf level (Asner, 1998; Roberts *et al.*, 2004). Within the NIR region, we found that leaf optical properties were consistently more directly expressed in deciduous dominated, high %N canopies. Given the strong correlation between % deciduous and canopy %N, we were able to narrow down our candidate structural traits to those that vary between broadleaf deciduous and needle-leaf evergreen species.

Presence of fine woody material (such as twigs) has been shown to enhance NIR absorption of canopies (Malenovsky *et al.*, 2008). Although we did not measure woody area index in this study, conifer stands tend to have more exposed woody components (Gower *et al.*, 1999), which may help to explain lower albedo of canopies dominated by conifer species. Malenovsky *et al.* (2008) pointed out, however, that wood is still a minor contributor to canopy reflectance compared to the amount of green foliage in the canopy. Typically the "amount" of green foliage in the canopy is reported on an area basis as LAI. Smolander and Stenberg (2003) have explained that changes in LAI in conifer canopies influences the probability of photons scattering multiple times, also called the photon recollision probability. Despite this, and several other modeling studies relating canopy reflectance to LAI (Chen and Leblanc, 1995; Jacquemond et al., 1995; Asner, 1998), recent field studies, as well as the current study, have found no

relationship between LAI and canopy albedo (Figure 9). Therefore, we attempted to explain patterns in NIR $F_{L\text{-}C}$ and albedo using other structural characteristics that hypothesized to influence photon recollision probability across a range in forest types.

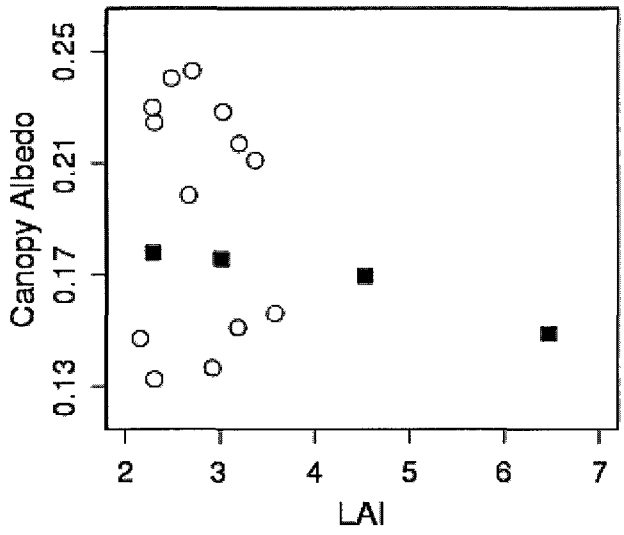

Figure 9 While many models incorporate LAI as a drive of canopy reflectance, recent studies (Ollinger et al., 2008; Hollinger et al., 2010) as well as the current study have found no relationship between canopy albedo and LAI at BDF (black squares) and BEF (open circles).

Recollision probability was originally defined by Smolander and Stenberg (2003) as the probability of a photon interacting with multiple needles in a single conifer shoot. Smolander and Stenberg (2005) proposed that recollision probability at the canopy level is related to the shoot recollision probability. They implied that recollision probability in broadleaved canopies was constant and lower than in coniferous canopies because self-shading will not occur within individual leaves. While this theory intuitively makes sense, it does not acknowledge that self-shading within canopies will occur not only between and within shoots in coniferous canopies, but also between leaves in broadleaved canopies due to leaf position (Ackerly, 1999). The extent to which self-shading occurs should be a function of the number and size (Ackerly and Bazzaz, 1995; Ackerly, 1999) and grouping of leaves (Chen and Leblanc, 1995), in addition to LAI, all of which vary in

broadleaved canopies, as well as across a range of forest compositions. The number of leaves per cubic meter fits well with these concepts. It is an aggregate variable calculated from canopy height, LAI, and leaf size. Increasing the number of leaves per cubic meter, particularly assuming no change in mean leaf size, would result in increased self-shading within a forest canopy, and therefore may influence scattering of light.

We used stepAIC to explore patterns of albedo and structural traits in our dataset. We found that canopy albedo was best explained by the number of leaves per cubic meter and CI (see Figure 10). These two variables make intuitive sense and are consistent with photon recollision probability theory. Increased clumping of canopy elements could affect light penetration into the canopy, and the number of leaves per cubic meter could influence how many times light scatters, with higher recollision probability in canopies with more leaves. Theoretically, the likelihood of any photon being absorbed within a canopy increases with the number of times that it interacts with canopy elements (Smolander and Stenberg, 2003), so deeper penetration and increased multiple scattering would result in lower albedo.

These data may provide an explanation for the relationship that has been observed and used in modeling studies between LAI and canopy reflectance in coniferous forests. If photon recollision probability is actually a function of the number of leaves per cubic meter, in homogeneous conifer canopies with little to no variation in mean leaf size, the number of leaves per cubic meter, and therefore photon recollision probability, would vary with LAI. It would require additional sampling in conifer and deciduous forests for analysis within forest types to support this hypothesis.

We also found that the number of leaves per cubic meter is correlated with canopy %N. Because of photosynthesis-N relations (Field and Mooney, 1986; Reich et al., 1997), there is a trade-off between the number of absorbers (i.e. leaves) and the

power of absorbers (i.e. foliar %N) in forest canopies. With lower concentrations of N in evergreen foliage, more leaves are required to meet the carbon costs of growth and competition in forests. The increased number of leaves could also cause increased scattering of incoming radiation and absorption. The effect of low foliar %N on forests is to increase the number of leaves to meet carbon costs, which in turn enhances absorption by decreasing the ability of photons to escape the canopy. Furthermore, clumping of foliage has been shown to increase carbon sequestration relative to unclumped canopies (Chen *et al.*, 2003). Clumping allows for radiation to penetrate further into canopies, decreasing the probability of photons escaping (Lewis and Disney, 2007), and therefore maximizing absorption. In addition to increasing canopy photosynthetic efficiency, increased absorption of radiation would also result in higher sensible and latent heat fluxes of forests (Bonan *et al.*, 2008), a potential evolutionary benefit to needle-leaved evergreen species of colder regions, which may help to extend short growing seasons and protect plants from damage or mortality.

Sources of Error

A component of external structure of evergreen needles may have been introduced in leaf albedo measurements. Needles were narrower and/or shorter than the size of the sampling window of the NIRS, so needle shape may have influenced scattering of incoming radiation, allowing for deeper penetration of radiation into and increased absorption of the sample of needles. Deciduous leaf samples were larger than the sampling window, so internal leaf compounds and structure were the only influence on absorption.

Uncertainties in estimates of LAI from digital hemispherical photography methods have been reported (Richardson *et al.*, 2011), as well as uncertainties in estimates of the associated CI (Chen, 1996). Repeatability of LAI estimates from this method have been questioned (Richardson *et al.*, 2011), partially due to sensitivity of the camera to light

conditions. For acceptable photographs, diffuse light conditions are necessary, and high contrast between foliage and sky depends on appropriate exposure of images (2 full stops over-exposed relative to open sky, Zhang *et al.*, 2005). Because of the amount of time associated with collecting photographs, changes in light conditions between photographs and between plots have been shown to affect estimates of LAI (Richardson *et al.*, 2011). In addition to systematic errors, uncertainties in estimates of CI, woody-to-total area ratio, and needle-to-total shoot area ratio have all been reported to have errors of approximately 10% (Chen, 1996).

One of the weaknesses of multiple regression analysis is that the number of candidate parameters, order of entry, and the algorithm used, can all affect the model, particularly when predictors are correlated (Whittingham *et al.*, 2006). Autocorrelation of variables in this dataset causes difficulties in determining a true model for predicting canopy albedo. It is possible that in reality, all canopy structural traits have some influence on canopy albedo because of roles in influencing light scattering, and the relationship between scattering and any give structural attribute may change based on changes in other structural attributes. Interactions between incoming radiation and forest canopies are quite complex, and may be influenced by any one of a number of traits. These data support the idea that many leaf and canopy traits converge, however, these results do not necessarily identify an answer to the structural driver of canopy albedo.

Conclusions

A goal of this study was to identify the underlying causes of the observed relationship between canopy albedo and %N. Interrelations between canopy structural attributes have prevented definitive findings, but instead provide support for the notion of convergence among multiple leaf and canopy properties that each have an effect on reflectance (Ollinger, 2011). Leaf and canopy %N and albedo correlate with many

structural attributes of forest canopies in New Hampshire, several of which have theoretical support from radiative transfer modeling studies. At the leaf level, we found that LMA correlates strongly with albedo, suggesting that changes in leaf structure that correlate with LMA, such as A_{MES}/A, may influence albedo. Leaf level drivers, in addition to structural traits of forest canopies that influence penetration and scattering of light affect the likelihood of absorption. In this study, we found a correlation between albedo and the number of leaves per cubic meter. This variable is a novel approach to measuring canopy structure that is consistent with photon recollision probability theory and should be considered for future radiative transfer modeling efforts.

Future studies should attempt to understand the extent to which multiple potential drivers influence albedo separately and in concert. In this study we investigated correlations between canopy %N, structure, and albedo in canopies that vary in forest composition. Efforts to parse the relative contributions of leaf and canopy optical and structural parameters to canopy albedo were confounded by interrelations among traits. Understanding the influences of different traits on canopy albedo, and how they respond to global change will help us to better predict reflectance of forest canopies in the future, and account for these changes in climate models and management efforts. Experimental approaches, while valuable for these purposes, are especially challenging because manipulations often influence forests in multiple ways on different time scales.

LITERATURE CITED

Aber JD. 1979. Foliage-height profiles and succession in northern hardwood forests. *Ecology* 60: 18-23.

Aber JD, J Amante, M Benander, B Godbois, B Oleksy, P Pellissier, A Reid and B Vangel. 2009. The forest resource at the Burley-Demerritt/Dudley-Bartlett Farm: Analysis as a potential source of renewable energy and bedding material for the organic dairy research farm. Unpublished research.

Ackerly D. 1999. Self-shading, carbon gain and leaf dynamics: a test of alternative optimality models. *Oecologia* 119: 300-310.

Ackerly DD and FA Bazzaz. 1995. Leaf dynamics, self-shading and carbon gain in seedlings of a tropical pioneer tree. *Oecologia* 101: 289-298.

Asner GP. 1998. Biophysical and biochemical sources of variability in canopy reflectance. *Remote Sensing of Environment* 64: 234-253.

Bala G, K Caldeira, M Wickett, TJ Phillips, DB Lobell, C Delire, and A Mirin. 2007. Combined climate and carbon-cycle effects of large-scale deforestration. *Proceedings of the National Academy of Sciences* 104: 6550-6555.

Bartlett MK, SV Ollinger, DY Hollinger, HF Wicklein, and AD Richardson. In Press. Canopy-scale relationships between foliar nitrogen and albedo are not observed in leaf reflectance and transmittance within temperate deciduous tree species. *American Journal of Botany.*

Bolster KL, ME Martin, and JD Aber. 1996. Determination of carbon fraction and nitrogen concentration in tree foliage by near infrared reflectance: a comparison of statistical method. *Canadian Journal of Forest Research* 101: 23,335-23,348.

Bonan GB. 2008. Forests and climate change: Forcings, feedbacks, and the climate benefits of forests. *Science 320*: 1444-1449.

Castro-Esau KL, Sanchez-Azofeifa GA, Rivard B, Wright AJ, and Quesada M. 2006. Variability in leaf optical properties of Mesoamerican trees and the potential for species classification. *American Journal of Botany* 94: 517-530.

Chen JM. 1996. Optically-based methods for measuring seasonal variation of leaf area index in boreal conifer stands. *Agricultural and Forest Meteorology* 80: 135-163.

Chen JM and J Cihlar. 1995. Quantifying the effect of canopy architecture on optical measurements of leaf area index using two gap size analysis methods. *IEEE Transactions on Geoscience and Remote Sensing* 33: 780-791.

Chen JM and SG Leblanc. 1997. A four-scale bidirectional reflectance model based on canopy architecture. *IEEE Transactions on Geoscience and Remote Sensing* 35: 1316-1337.

Chen JM, CH Menges, and SG Leblanc. 2005. Global mapping of foliage clumping index using multi-angular satellite data. *Remote Sensing of Environment* 97: 447-457.

Chen JM, J Liu, SG Leblanc, R Lacaze and JL Roujean. 2003. Multi-angular optical remote sensing for assessing vegetation structure and carbon absorption. *Remote Sensing of Environment* 84: 516-525.

Close DC and CL Beadle. 2006. Leaf angle responds to nitrogen supply in eucalypt seedlings. Is it a photoprotective mechanism? *Tree Physiology* 26: 743-748.

Field C and HA Mooney. The photosynthesis-nitrogen relationship in wild plants. *On the Economy of Plant Form and Function*. 2nd Edition. Ed. Thomas Givnish. Cambridge University Press, 1986, 25-49.

Forseth IN and AH Teramura. 1986. Kudzu leaf energy budget and calculated transpiration: the influence of leaflet orientation. *Ecology* 67: 564-571.

Gates DM, HJ Keegan, JC Schleter, and VR Weidner. 1965. Spectral properties of plants. *Applied Optics* 4: 11-21.

Gerard FF and PRJ North. 1997. Analyzing the effect of structural variability and canopy gaps on forest BRDF using a geometric-optical model. *Remote Sensing of Environment* 62: 46-62.

Gower ST, CJ Kucharik, JM Norman. 1999. Direct and indirect estimation of leaf area index, f_{APAR}, and net primary production of terrestrial ecosystems. *Remote Sensing of Environment* 70: 29-51.

Hollinger DY. 1996. Optimality and nitrogen allocation in a tree canopy. *Tree Physiology* 16: 627-634.

Hollinger DY, SV Ollinger, AD Richardson, TP Meyers, DB Dail, ME Martin, NA Scott, TJ Arkebauer, DD Baldocchi, KL Clark, PS Curtis, KJ Davis, AR Desai, D Dragoni, ML Goulden, L Gu, GG Katul, SG Pallardy, KT Paw U, HP Schmid, PC Stoy, AE Suyker and SB Verma. 2010. Albedo estimates for land surface models and support for a new paradigm based on foliage nitrogen concentration. *Global Change Biology* 16: 696-710.

Jacquemoud S. 1993. Inversion of the PROSPECT + SAIL canopy reflectance model from AVIRIS equivalent spectra: Theoretical study. *Remote Sensing of Environment* 44: 281-292.

Jacquemoud S and F Baret. 1990. PROSPECT: A model of leaf optical properties spectra. *Remote Sensing of Environment* 34: 75-91.

Jacquemoud S, F Baret, B Andrieu, FM Danson and K Jaggard. 1995. Extraction of vegetation biophysical parameters by inversion of the PROSPECT + SAIL models on sugar beet canopy reflectance data. Application to TM and AVIRIS sensors. *Remote Sensing of Environment* 52: 163-172.

James SA, WK Smith and TC Vogelmann. 1999. Ontogenetic differences in mesophyll structure and chlorophyll distribution in *Eucalyptus globulus* ssp. *globulus* (*Myrtaceae*). *American Journal of Botany* 86: 198-207.

Johnson LF. 2001. Nitrogen influence on fresh-leaf NIR spectra. *Remote Sensing of Environment* 78: 314-320.

Leak WB and M-L Smith. 1996. Sixty years of management and natural disturbance in a New England forested landscape. *Forest Ecology and Management* 81: 63-73.

Leblanc SG. 2006. Digital Hemispherical Photography Manual. Natural Resources Canada.

Lepine LC, SV Ollinger, ME Martin, FB Sullivan and J Xiao. In prep. Variability in albedo and canopy structural properties along disturbance-recovery gradients in Canadian evergreen needleleaf forests.

Lewis P and M Disney. 2007. Spectral invariants and scattering across multiple scales from within-leaf to canopy. *Remote Sensing of Environment* 109: 196-206.

Malenovksy Z, E Martin, L Homolova, J-P Gastellu-Etchegorry, R Zurita-Milla, ME Schaepman, R Pokorny, JGPW Clevers, and P Cudlin. 2008. Influence of woody elements of a Norway spruce canopy on nadir reflectance simulated by the DART model at very high spatial resolution. *Remote Sensing of Envrionment* 112: 1-18.

Martin ME, SD Newman, JD Aber, and RG Congalton. 1997. Determining forest species composition using high spectral resolution remote sensing data. *Remote Sensing of Envrionment* 65: 249-254.

Niinemets U. 1999. Components of leaf dry mass per area – thickness and density – alter leaf photosynthetic capacity in reverse directions in woody plants. *New Phytologist* 144: 35-47.

Niinemets U. 2001. Global-scale climatic controls of leaf dry mass per area, density, and thickness in trees and shrubs. *Ecology* 82: 453-469.

Niinemets U, A Cescatti, A Lukjanova, M Tobias, and L Truss. 2002. Modification of light-acclimation of Pinus sylvestris shoot architecture by site fertility. *Agricultural and Forest Meteorology* 111: 121-140.

Ollinger SV. 2011. Sources of variability in canopy reflectance and the convergent properties of plants. *New Phytologist* 189: 375-394.

Ollinger SV, JD Aber, CA Federer, GM Lovett and J Ellis. 1995. Modeling physical and chemical climatic variables across the northeastern US for a Geographic Information System. USDA Forest Service General Technical Report NE-191.

Ollinger SV, AD Richardson, ME Martin, DY Hollinger, SE Frolking, PB Reich, LC Plourde, GG Katul, JW Munger, R Oren, ML Smith, KT Paw U, PV Bolstad, BD Cook, MC Day, TA Martin, RK Monson, and HP Schmid. 2008. Canopy nitrogen, carbon assimilation and albedo in temperate and boreal forests: functional relations and potential climate feedbacks. *Proceedings of the National Academy of Sciences* 105: 19335–19340.

Ollinger SV and ML Smith. 2005. Net primary production and canopy nitrogen in a temperate forest landscape: An analysis using imaging spectroscopy, modeling and field data. *Ecosystems* 8: 760-778.

Oker-blom P and S Kellomaki. 1983. Effect of grouping of foliage on the within-stand and within-crown light regime: comparison of random and grouping canopy models. *Agricultural Meteorology* 28: 143-155.

Parker GG, JP O'Neill and D Higman. 1989. Vertical profile and canopy organization in a mixed deciduous forest. *Vegetatio* 85: 1-11.

Rautiainen M, P Stenberg, T Nilson, and A Kuusk. 2004. The effect of crown shape on the reflectance of coniferous stands. *Remote Sensing of Environment* 89: 41-52.

Rautiainen M and P Stenberg. 2005. Application of photon recollision probability in coniferous canopy reflectance simulations. *Remote Sensing of Environment* 96: 98-107.

Reich PB, BD Kloeppel, DS Ellsworth, and MB Walters. 1995. Different photosynthesis-nitrogen relations in a deciduous hardwood and evergreen coniferous tree species. *Oecologia* 104: 24-30.

Reich PB, MB Walters, and DS Ellsworth. 1997. From tropics to tundra: Global convergence in plant functioning. *Proceedings of the National Academy of Sciences* 94: 13730-13734.

Richardson AD, DB Dail and DY Hollinger. 2011. Leaf area index uncertainty estimates for model-data fusion applications. *Agricultural and Forest Meteorology* 151: 1287-1292.

Roberts DA, SL Ustin, S Ogunjemiyo, J Greenberg, SZ Dobrowski, J Chen, and TM Hinckley. 2004. Spectral and structural measures of northwest forest vegetation at leaf to landscape scales. *Ecosystems* 7: 545-562.

Serrano L. 2008. Effects of leaf structure on reflectance estimates of chlorophyll content. *International Journal of Remote Sensing* 29: 5265-5274.

Shipley B, MJ Lechowicz, IJ Wright, PB Reich. 2006. Fundamental trade-offs generating the worldwide leaf economics spectrum. *Ecology* 87: 535-541.

Slaton MR, ER Hunt Jr. and WK Smith. 2001. Estimating near-infrared leaf reflectance from leaf structural characteristics. *American Journal of Botany* 88: 278-284.

Smith ML and ME Martin. 2001. A plot-based method for rapid estimation of forest canopy chemistry. *Canadian Journal of Forest Research* 31: 549-555.

Smolander S and P Stenberg. 2003. A method to account for shoot scale clumping in coniferous canopy reflectance models. *Remote Sensing of Environment* 88: 363-373.

Smolander S and P Stenberg. 2005. Simple parameterizations of the radiation budget of uniform broadleaved and coniferous canopies. *Remote Sensing of Environment* 94: 355-363.

Thomas QR, CD Canham, KC Weathers, and CL Goodale. 2010. Increased tree carbon storage in response to nitrogen deposition in the US. *Nature Geoscience* 3: 13-17.

Thompson C, J Beringer, FS Chapin III and AD McGuire. 2004. Structural complexity and land-surface energy exchange along a gradient from arctic tundra to boreal forest. *Journal of Vegetation Science* 15: 397-406.

Thompson M, D Adams and KN Johnson. 2009. The albedo effect and forest carbon offset design. *Journal of Forestry* 107: 425-431.

Verhoef W. 1984. Light scattering by leaf layers with application to canopy reflectance modeling: The SAIL model. *Remote Sensing of Environment* 16: 125-141.

Whitehead D, JC Grace, and MJS Godfrey. 1990. Architectural distribution of foliage in individual Pinus radiata D. Don crowns and the effects of clumping on radiation interception. *Tree Physiology* 7: 135-155.

Whittingham MJ, PA Stephens, RB Bradbury and RP Freckleton. 2006. Why do we still use stepwise modeling in ecology and behavior? *Journal of Animal Ecology* 75: 1182-1189.

Wicklein HF, SV Ollinger, ME Martin, DY Hollinger, LC Lepine, MC Day, MK Bartlett, AD Richardson, RJ Norby. In review. Variation in foliar nitrogen and albedo in response to nitrogen fertilization and elevated CO2. *Oecologia*.

Wright IJ, PB Reich, M Westoby, DD Ackerly, Z Baruch, F Bongers, J Cavender-Bares, T Chapin, JHC Cornelissen, M Diemer, J Flexas, E Garnier, PK Groom, J Gulias, K Hikosaka, BB Lamont, T Lee, W Lee, C Lusk, JJ Midgley, ML Navas, U Niinemets, J Oleksyn, N Osada, H Poorter, P Poot, L Prior, VI Pyankov, C Roumet, SC Thomas, MG Tjoelker, EJ Veneklaas, and R Villar. 2004. The worldwide leaf economics spectrum. *Nature* 428: 821-827.

Zhang Y, JM Chen and JR Miller. 2005. Determining digital hemispherical photograph exposure for leaf area index estimation. *Agricultural and Forest Meteorology* 133: 166-181.